Supporting Information

Synthesis of electronically modified carbon nitride from a processable semiconductor, 3-aminotriazole-1,2,4 oligomer, *via* a topotactic-like phase transition

*Aleksandr Savateev, Sergey Pronkin, Jan Dirk Epping, Marc Georg Willinger, Markus Antonietti, and Dariya Dontsova**

Chemicals. 3-aminotriazole-1,2,4 (96%) and triethanolamine (TEOA, 98%) were purchased from Alfa Aesar; ammonium persulfate (for analysis) – from AppliChem; hexachloroplatinic acid (H_2PtCl_6, 8 wt. % aqueous solution) – from Sigma Aldrich.

Characterization

Hydrogen evolution reactions (HER). HER were performed using a side-irradiated closed steel reactor equipped with a Teflon inlet, thermocouple, pressure sensor, magnetic stirring and thermostat, and connected to a Schlenk manifold. In all the cases, Pt and triethanolamine (TEOA) were used as a co-catalyst for hydrogen generation and as a sacrificial hole-scavenger, respectively. In addition, being a good buffering agent, TEOA provides stable pH of 10.8 for the whole duration of the experiment. Pt was in-situ photo-deposited onto tested photocatalysts using hexachloroplatinic acid (H_2PtCl_6) as a precursor. During the experiment, the buildup of pressure was monitored as a function of the irradiation time. A 50 W white LED array was used as an energy efficient irradiation source.

Hydrogen evolution set up and measurement procedure. All catalytic experiments were carried out under argon atmosphere. The double walled and thermostatically controlled reaction vessel was connected to a digital pressure sensor (Type-P30, DP = 0.1%, WIKA Alexander Wiegand SE & Co. KG, Germany) to monitor the pressure increase due to hydrogen evolution. 50 mg of sample were placed inside the reactor. Then the reactor was evacuated and refilled with argon for several times. H_2O and TEOA were pre-treated before use. H_2O was degassed first for 1 h under vacuum in an ultrasonic bath and followed by purging with argon for 1 h. TEOA at vigorously stirred in vacuum (0.05 torr) for 1 h and then purged for 1 h with argon. The solvent mixture (38 mL), composed of water and triethanolamine (TEOA) in the ratio of 9/1 (v/v) and 39.4 μL H_2PtCl_6 solution (corresponds to theoretical 3 wt. % of Pt loading onto the catalyst), were added, and the temperature was maintained at 25 °C by a thermostat. After stirring for 10 min to reach thermal equilibrium, the reaction was started by switching on 50 W white LED array (Bridgelux BXRA-50C5300, $\lambda > 410$ nm). The amount of evolved gas was continuously monitored by means of the time dependent pressure increase. The hydrogen evolution rate was calculated according to the Ideal Gas law:

$$\dot{n} = \frac{n}{t} = 10^5 \frac{\Delta p \cdot V}{R \cdot T \cdot t}$$

where n is hydrogen evolution rate [μmol/h], n moles hydrogen [μmol] , t - illumination time [h], Δp - pressure increase [bar] during irradiation time t, V - volume headspace above reaction solution, R - universal gas constant [8.314 J/(mol·K)] and T - temperature [298 K].

To confirm that the evolved gas is hydrogen, the headspace of the reactor after the test was analyzed using gas chromatography mass spectrometry (SHIMADZU GCMS-QP2010; using argon as a carrier gas).

Powder X-Ray diffraction patterns were measured on a Bruker D8 Advance diffractometer equipped with a scintillation counter detector with CuK_α radiation ($\lambda = 0.15418$ nm) applying 2θ step size of 0.05° and counting time of 3s per step. FT-IR spectra were recorded on a Varian1000 FT-IR spectrometer equipped with an attenuated total reflection unit applying a resolution of 2 cm^{-1}. Nitrogen adsorption/desorption measurements were performed after degassing the samples at 150 °C for 20 hours using a Quantachrome Quadrasorb SI-MP porosimeter at 77.4 K. The specific surface areas were calculated by applying the Brunauer-Emmett-Teller (BET) model to adsorption isotherms for $0.05 < p/p0 < 0.3$ using the QuadraWin 5.05 software package. Elemental analysis (EA) was accomplished as combustion analysis using a Vario Micro device. Scanning electron microscopy (SEM) images were obtained on a LEO 1550-Gemini microscope. Transmission electron microscopy (TEM) was performed on a CM200FEG (Philips) microscope, operated at 200 kV. Samples were prepared by depositing a drop of a suspension of particles in ethanol onto the amorphous carbon film. Optical absorbance spectra of powders were measured on a Shimadzu UV 2600 equipped with an integrating sphere. The emission spectra were recorded on LS-50B, Perkin Elmer instrument. The excitation wavelength was 350 nm. EDX investigations were conducted on a Link ISIS-300 system (Oxford Microanalysis Group) equipped with a Si(Li) detector and an energy resolution of 133 eV.

Mott-Schottky analysis was performed by measuring impedance spectra of the samples in a potential range from 0.40 to -0.60 V RHE, -0.02 V potential step, and frequencies from 10 kHz to 0.1 Hz, 7 mV potential amplitude. The measurements were performed in a standard three-compartment electrochemical cell. Pt coil and mercury sulfate electrodes were utilized as counter and reference electrodes correspondingly. The curves are presented in reversible hydrogen electrode scale RHE. (0.000 V RHE = -0.635 V Ag/AgCl for pH=7.0). The measurements were performed in 0.1 M phosphate buffer solution with pH=7.0. The solution was purged by nitrogen gas before the measurements to remove oxygen; constant flow of nitrogen gas was kept during the measurements in order to avoid oxygen leaking into the cell.

The electrodes were prepared by deposition of known amount of the powder on an Au substrate. Au was chosen as a substrate electrode due to 1) its low interfacial capacity comparing to other typical substrates, such as carbon or metal oxides (ITO, FTO), 2) high surface roughness and 3) positive surface charge helping to improve the adhesion of powder samples, whose surface is negatively-charged. In order to prepare the electrode the known amount of powder was ultrasonically dispersed in ethanol in order to make 100 mg/ml ink. Then 100 µl of ink was deposited on the Au substrate in 5 steps with drying in air between the steps. Finally, 40 µl of 5% solution of Nafion in ethanol was pipetted on the deposit to avoid its detachment. Preliminary experiments with pure Au substrate and Au+Nafion electrode were performed to demonstrate their negligible contribution into the measured capacity of electrodes with deposited samples powder.

Measured impedance spectra were fitted with the simplest equivalent circuit capable to fit experimental data: $R_1(CR_2)$. Here R_1 is related to the resistance of the electrolyte, R_2 is charge transfer resistance due to reduction of residual oxygen and/or evolution of hydrogen (close

and below 0,00 V RHE), C is an interfacial capacity predominantly determined by space charge layer in the semiconducting electrode.[1] In order to take into account frequency dispersion of C due to surface inhomogeneity, the capacity was modelled as constant phase element Q ($-Z''=1/C(j\cdot\omega)^{\alpha}$) with fixed phase shift constant $\alpha=0,90$.

Solid state NMR spectra were recorded with a Bruker Avance 400 MHz spectrometer operating at 100.56 MHz for ^{13}C, 40.53 MHz for ^{15}N and 399.88 MHz for ^{1}H. ^{1}H-^{13}C and ^{1}H-^{15}N cross polarization magic angle spinning (CP-MAS) NMR experiments were carried out at a MAS rate of 10 kHz using a 4 mm MAS HX double resonance probe. The ^{1}H $\pi/2$ pulse length was 3.1 µs and two pulse phase modulation (TPPM) heteronuclear dipolar decoupling was used during acquisition. The spectra were measured using contact time of 2.0 ms for ^{13}C and 4.0 ms for ^{15}N and recycle delays of 2 s and 5 s, respectively. All ^{13}C spectra are referenced to external TMS at 0 ppm using adamantane as a secondary reference. All ^{15}N spectra are referenced to neat nitromethane CH_3NO_2 at 0 ppm using solid NH_4Cl as a secondary reference.

TGA-MS measurements were performed using a thermo microbalance TG 209 F1 Libra (Netzsch, Selb, Germany) coupled with a Thermostar Mass spectrometer GSD 301 T3 (Pfeiffer Vacuum; Asslar/Germany). The ionization was by electron impact using an iridium filament as ion source; ionization energy was 75 eV, and ions were separated in a quadrupole mass filter. A platinum crucible was used for the measurement of 10±1mg of samples in a helium flow of $10mL\cdot min^{-1}$ and a purge flow of $10mL\cdot min^{-1}$. Data were analyzed using Proteus (6.0.0) and Quadstar (7.03) software packages. Prior to analysis, the sample was degassed at 150 °C and 0.01 mbar for 20 hours to remove the surface adsorbed water.

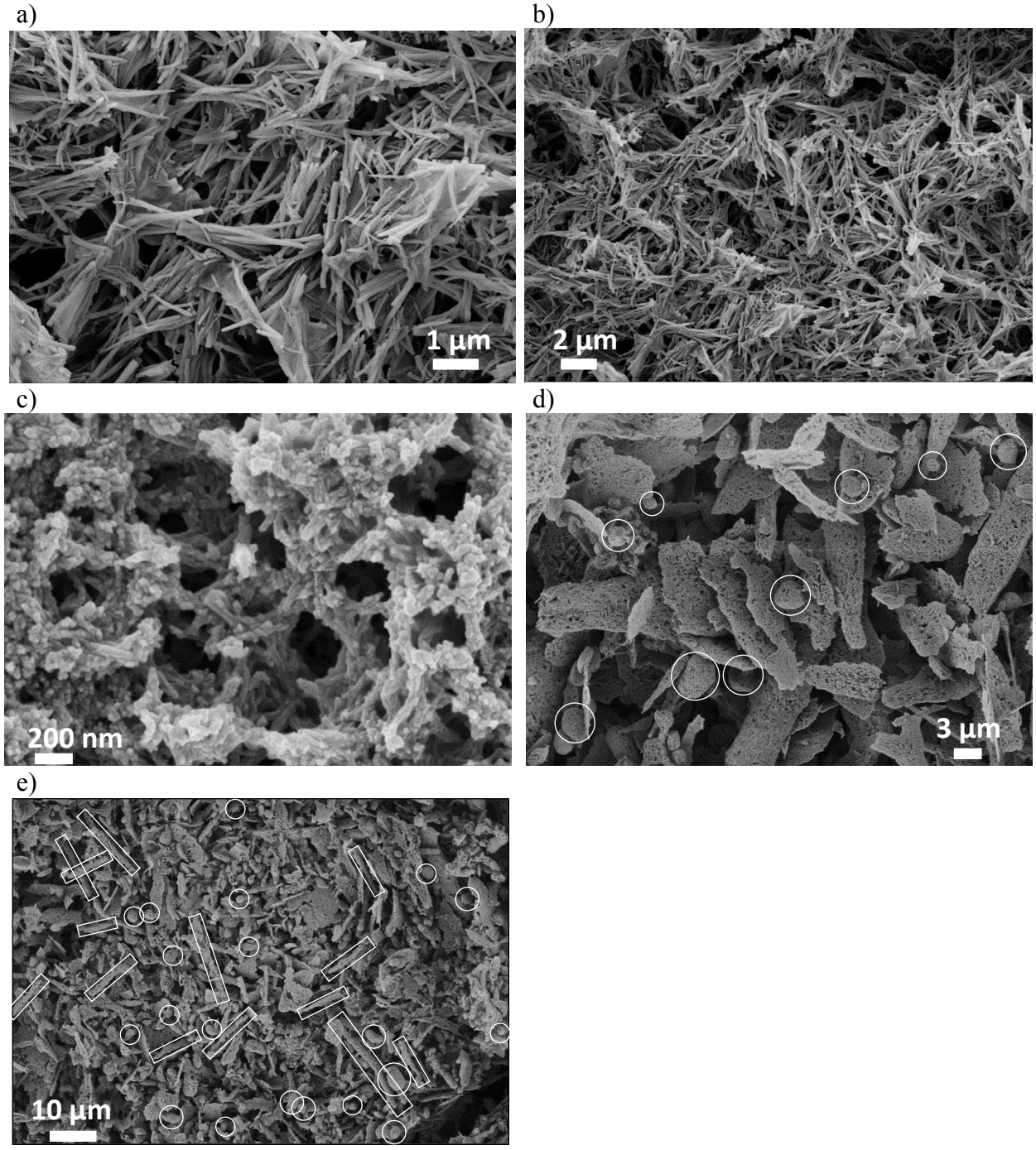

Figure S1. SEM images of OATA-2 (a,b), OATA-3 (c), and OATA-4 containing eye guiding marks that highlight nanoparticle agglomerates (d,e).

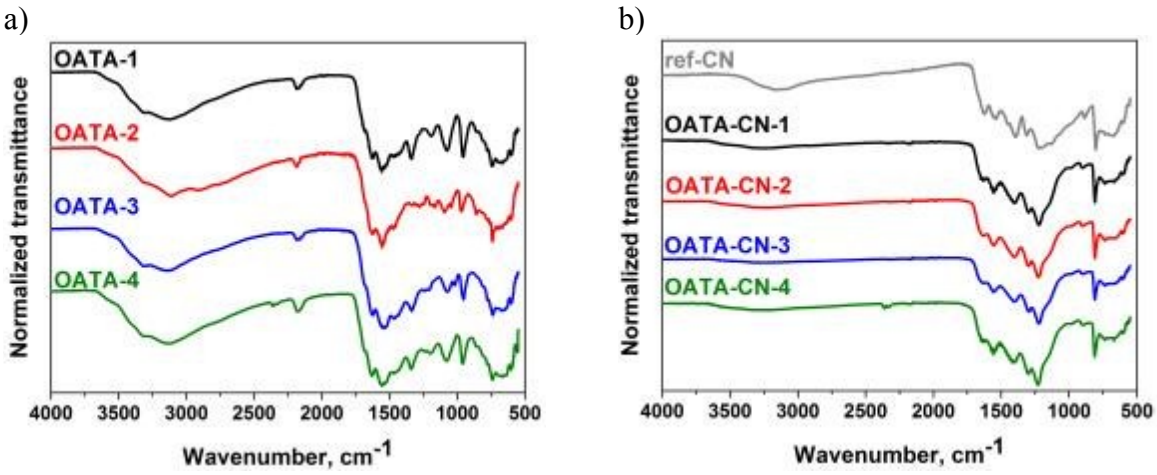

Figure S2. FTIR-ATR spectra of OATA precursors (a) and OATA-CN-N products (b).

Table S1. Elemental composition of OATA-N and OATA-CN-N as determined by elemental analysis (C, N, H) and energy-dispersive X-ray spectroscopy (O, S, Cl content).

Entry	Name	Description	C, wt. %	N, wt. %	H, wt. %	O, wt. %	S, wt. %	Cl, wt. %	C/N ratio
	$C_8N_{16}H_8$ theoretical	calc. for the structure shown in Figure 1a	26.27	68.27	2.46	-	-	-	0.429
1	OATA-1	Prepared using NH_4OH	26.56	61.05	3.45	8.94	0.00	0.00	0.435
2	OATA-2	Prepared using KOH	27.02	58.80	3.26	10.92	0.00	0.00	0.459
3	OATA-3	Precipitated from DMSO solution	27.50	57.80	3.44	11.26	0.00	0.00	0.476
4	OATA-4	OATA-1 freeze-dried	25.58	53.28	3.44	17.70	0.00	0.00	0.480
5	g-CN	reference sample prepared from melamine	34.87	60.53	2.00	2.60	0.00	0.00	0.576
6	OATA-CN-1	Precursor: OATA-1	35.44	58.79	2.69	3.07	0.00	0.00	0.603
7	OATA-CN-2	Precursor: OATA-2	35.79	58.98	2.27	2.96	0.00	0.00	0.607
8	OATA-CN-3	Precursor: OATA-3	36.31	58.32	2.27	3.10	0.00	0.00	0.623
9	OATA-CN-4	Precursor: OATA-4	35.81	58.72	2.65	2.82	0.00	0.00	0.610

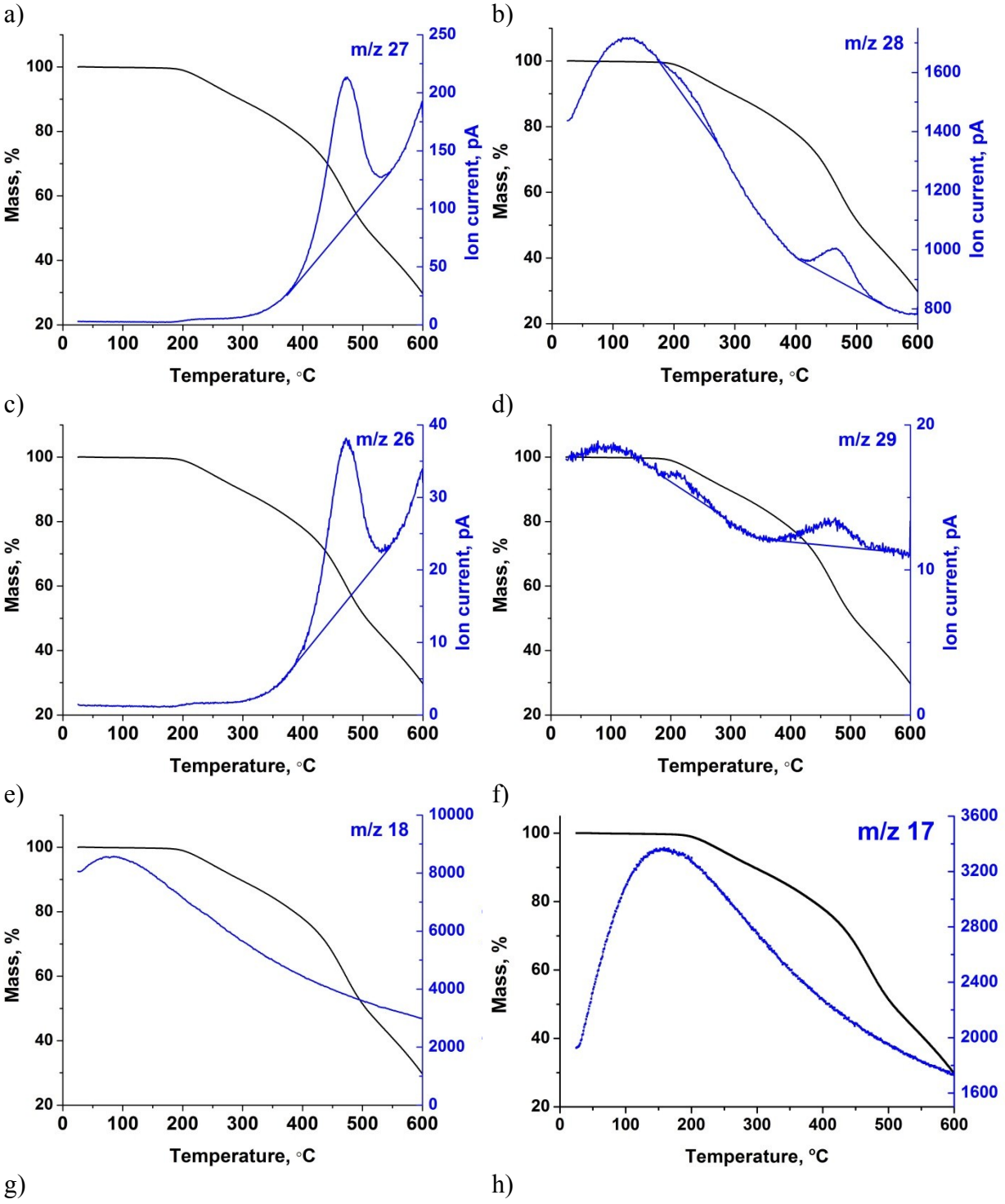
a)
m/z 27
Mass, %
Ion current, pA
Temperature, ◦C
b)
m/z 28
Mass, %
Ion current, pA
Temperature, ◦C
c)
m/z 26
Mass, %
Ion current, pA
Temperature, ◦C
d)
m/z 29
Mass, %
Ion current, pA
Temperature, ◦C
e)
m/z 18
Mass, %
Temperature, ◦C
f)
m/z 17
Mass, %
Temperature, °C
g)
h)

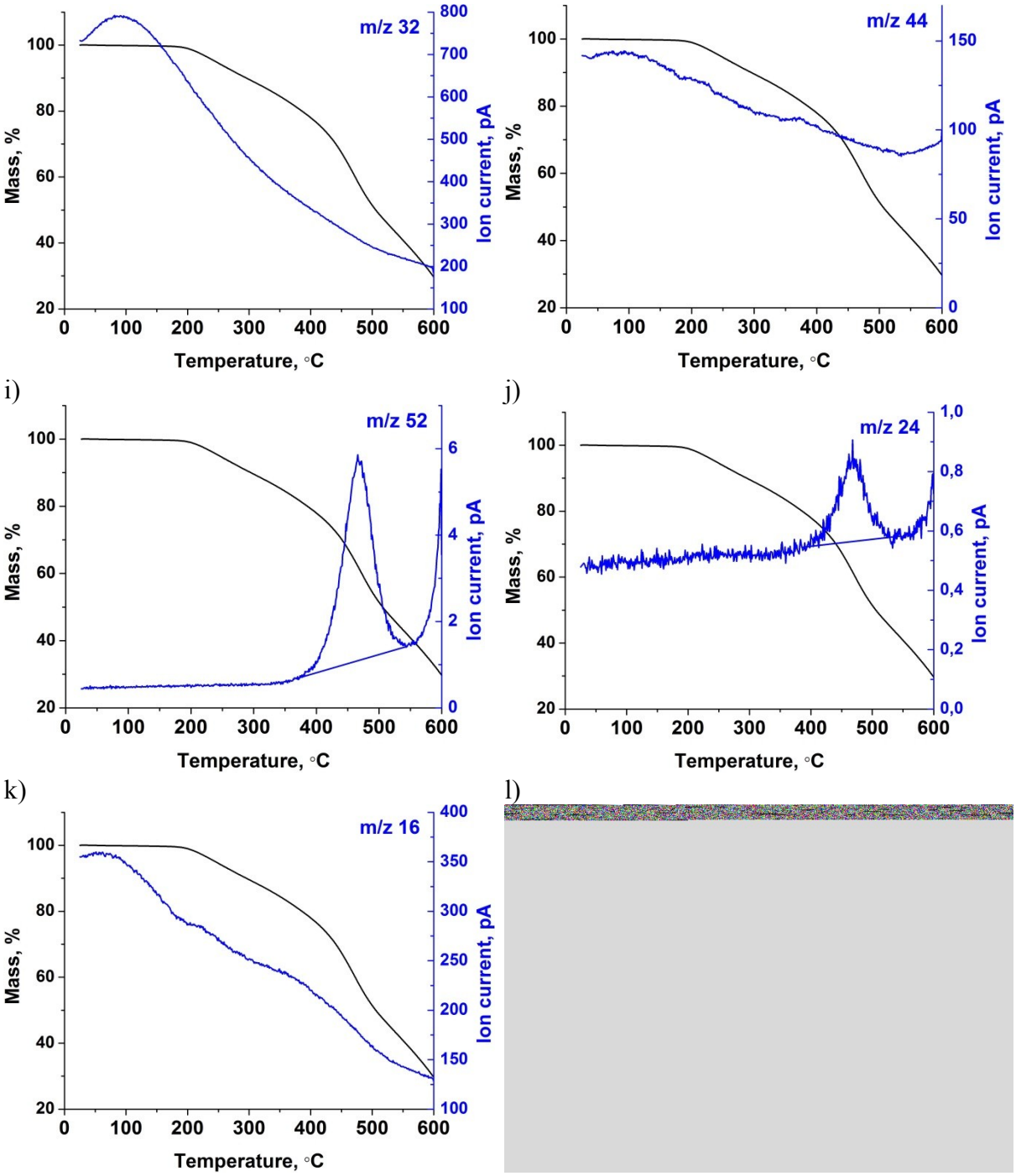

Figure S3. TGA and MS ion current curves for the selected mass numbers measured for OATA-1 sample. Analysis was performed using He as a carrier gas. Carrier gas contains ≤ 2.0 ppm water, ≤ 2.0 ppm oxygen, ≤ 0.2 ppm hydrocarbons, ≤ 5.0 ppm nitrogen.

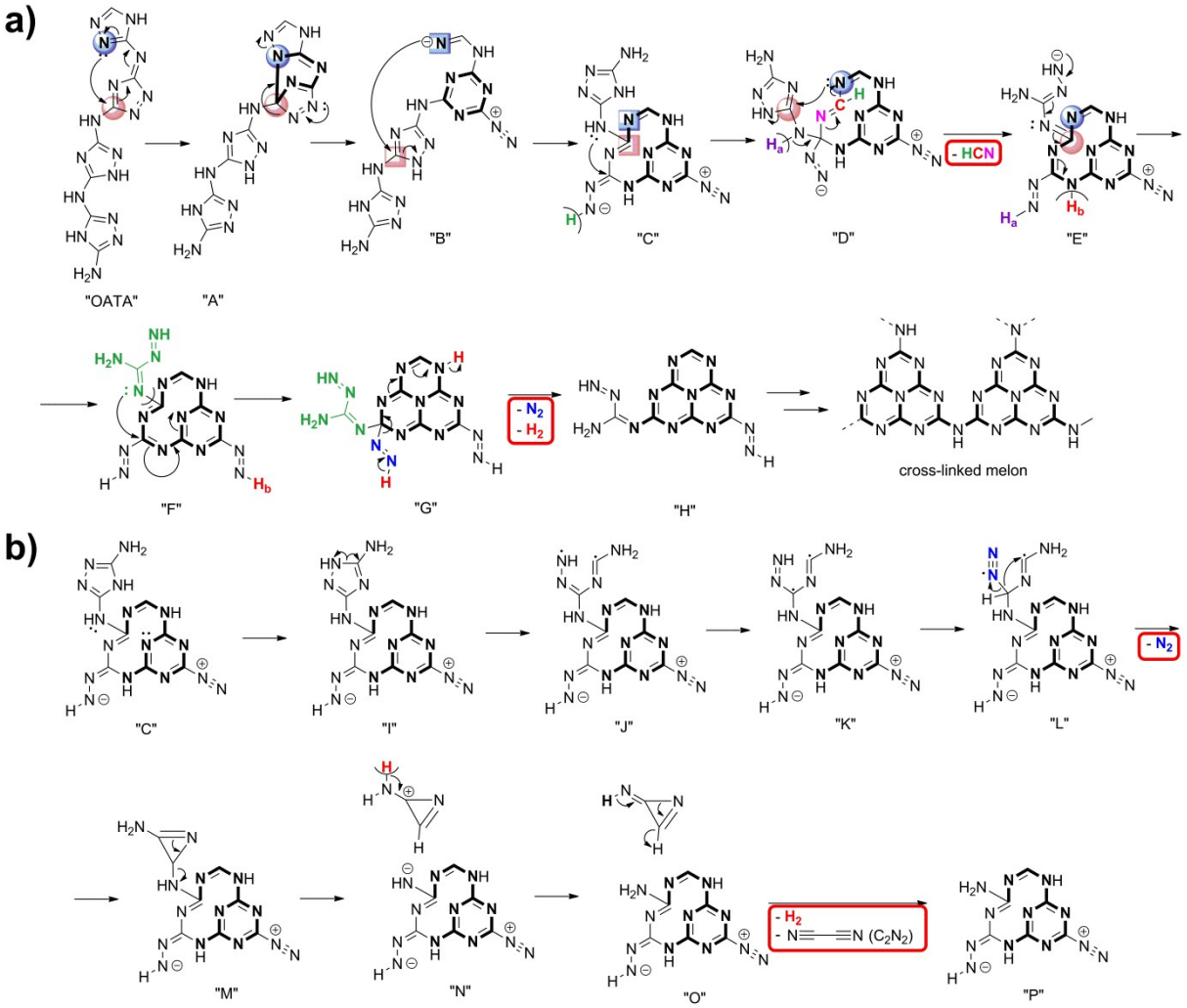

Figure S4. a) A possible mechanism of tri-*s*-triazine ring formation from OATA. Nucleophiles involved at particular step are highlighted in blue color while electrophiles in red. Small molecules that are expelled during the synthesis are shown in red rectangles. b) A possible mechanism of C_2N_2 formation.

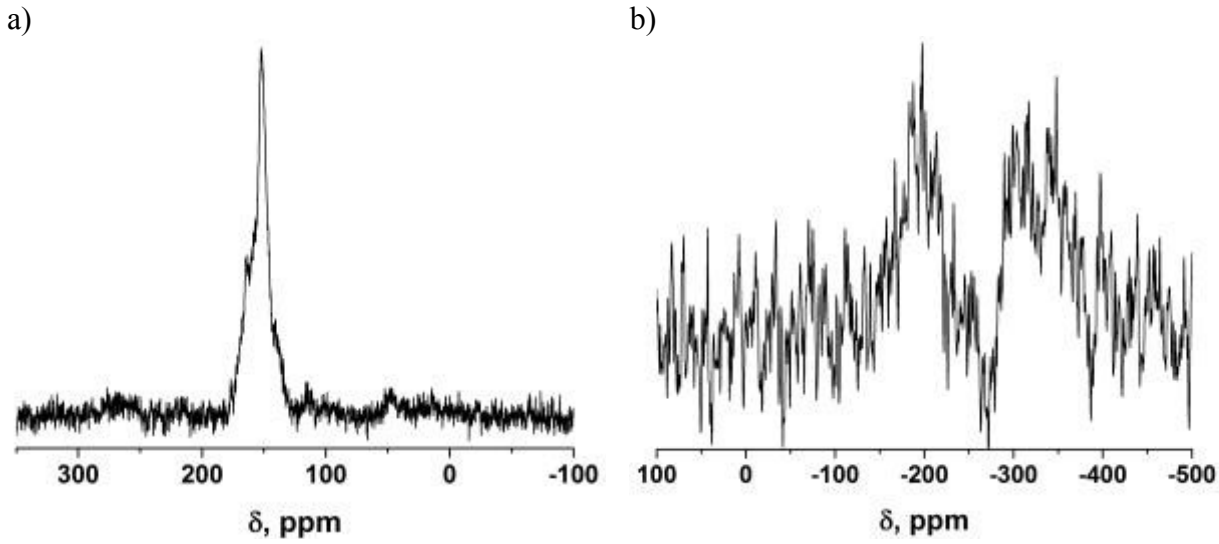

Figure S5. ^{13}C (a) and ^{15}N (b) CP-MAS NMR spectra of OATA.

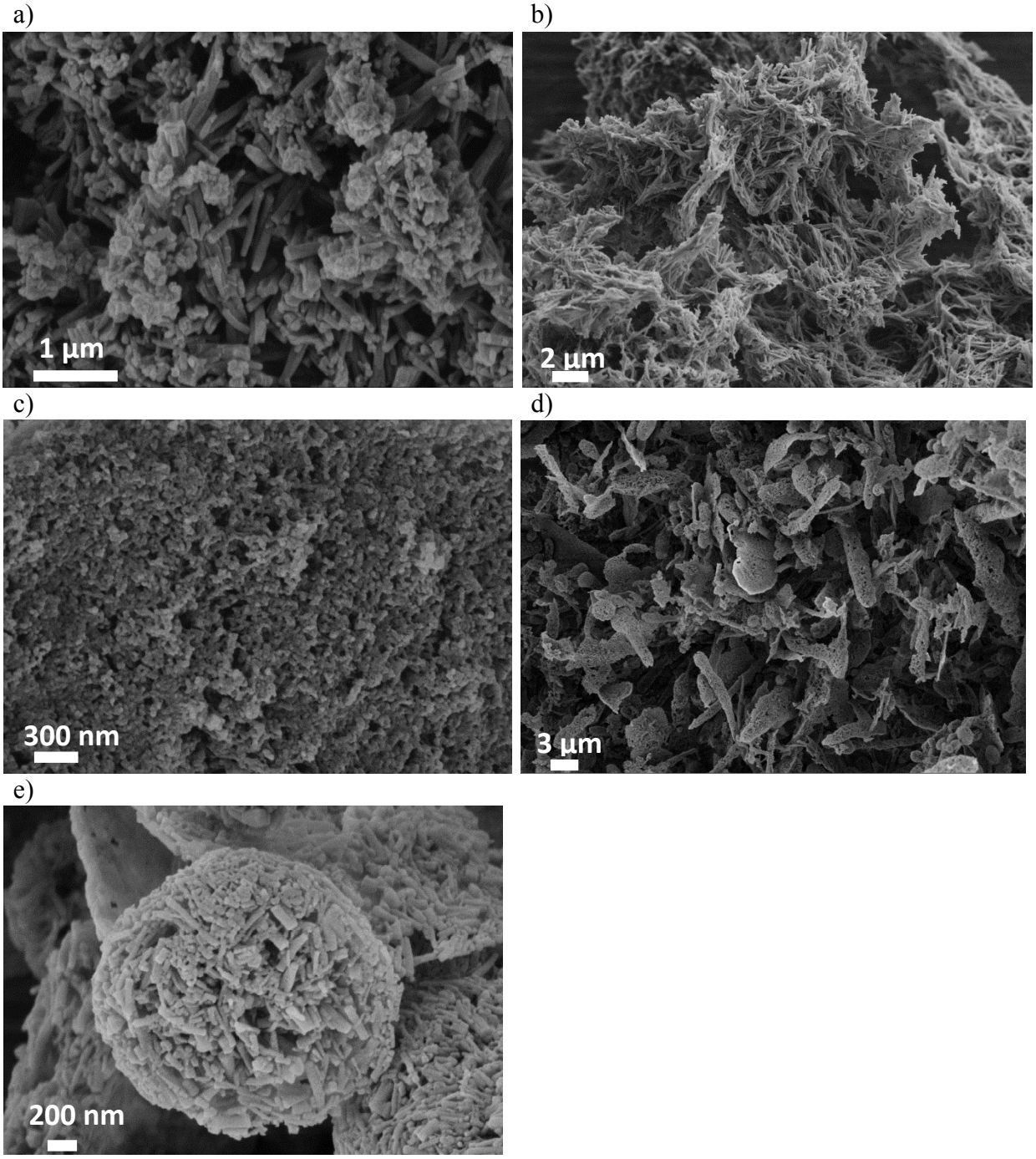

Figure S6. SEM images of OATA-CN-1 (a), OATA-CN-2 (b), OATA-CN-3 (c) and OATA-CN-4 (d, e).

Table S2. Sorption, optical and photocatalytic properties of OATA precursors and OATA-CN products.

Entry	Name	Surface area, m^2/g	Optical band gap, eV	Activity in HER, $\mu mol(H_2)/h$
1	OATA-1	38	1.76	0.00
2	OATA-2	28	1.84	n/a
3	OATA-3	89	1.92	n/a
4	OATA-4	43	n/a	n/a
5	OATA-CN-1	38	2.23	3.21
6	OATA-CN-2	28	2.23	2.66
7	OATA-CN-3	66	2.17	3.17
8	OATA-CN-4	35	2.23	1.10
9	ref-CN	8	2.75	0.66

n/a – not analyzed

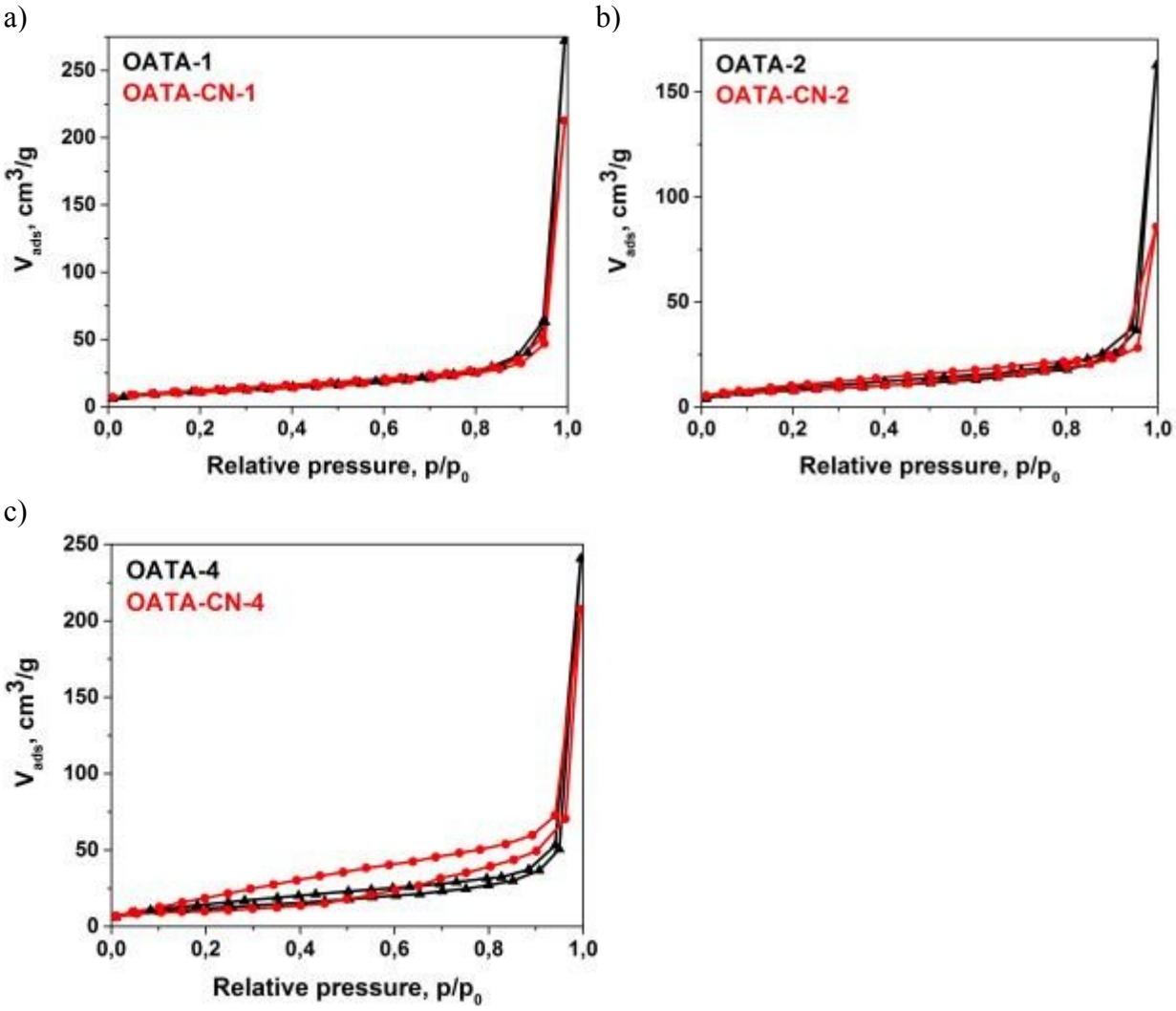

Figure S7. N_2 sorption isotherms of OATA and OATA-CN materials.

a) b)

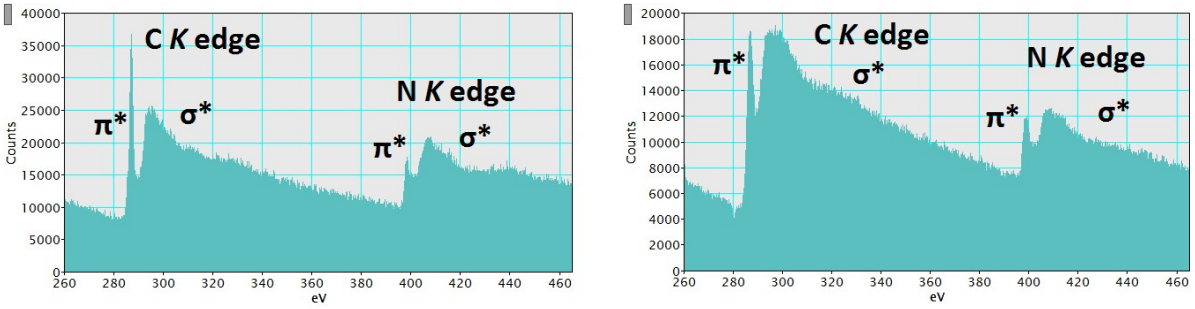

Figure S8. EEL spectra of OATA-CN-3: a) first measurement, b) second measurement of the same region.

a) b)

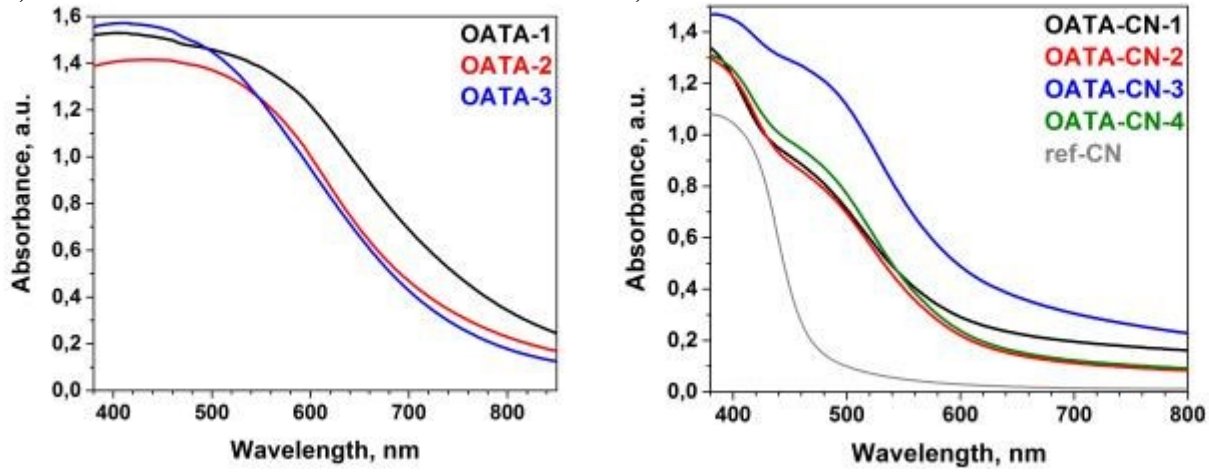

Figure S9. UV-Vis absorption spectra of OATA-N (a) and OATA-CN-N materials compared to ref-CN (b).

a) b)

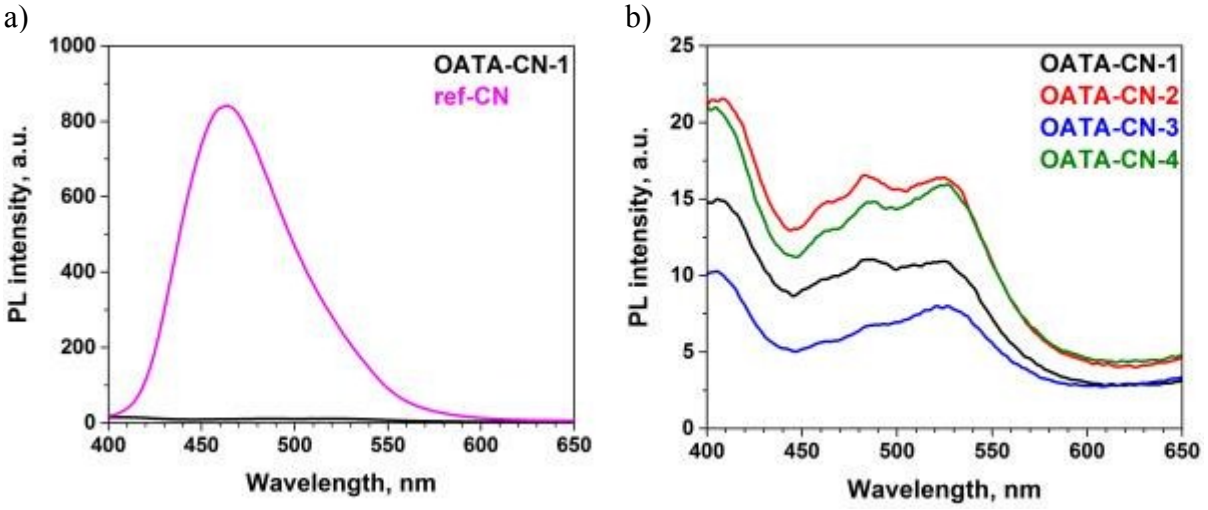

Figure S10. Steady state photoluminescence spectra of ref-CN compared to OATA-CN-1 (a) and those of OATA-CN-N materials (b).

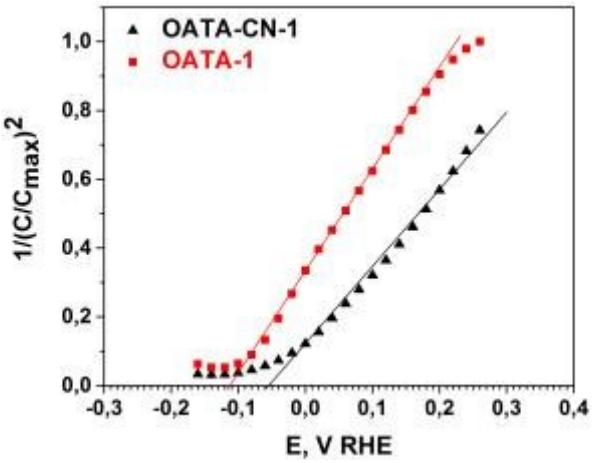

Figure S11. Mott-Schottky plot of OATA-1 and OATA-CN-1.

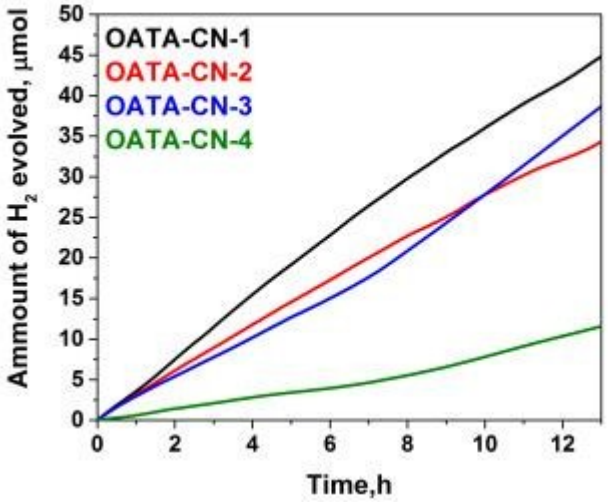

Figure S12. Time dependent Pt-assisted HER using TEOA as a sacrificial holes scavenger (white LED 50W).

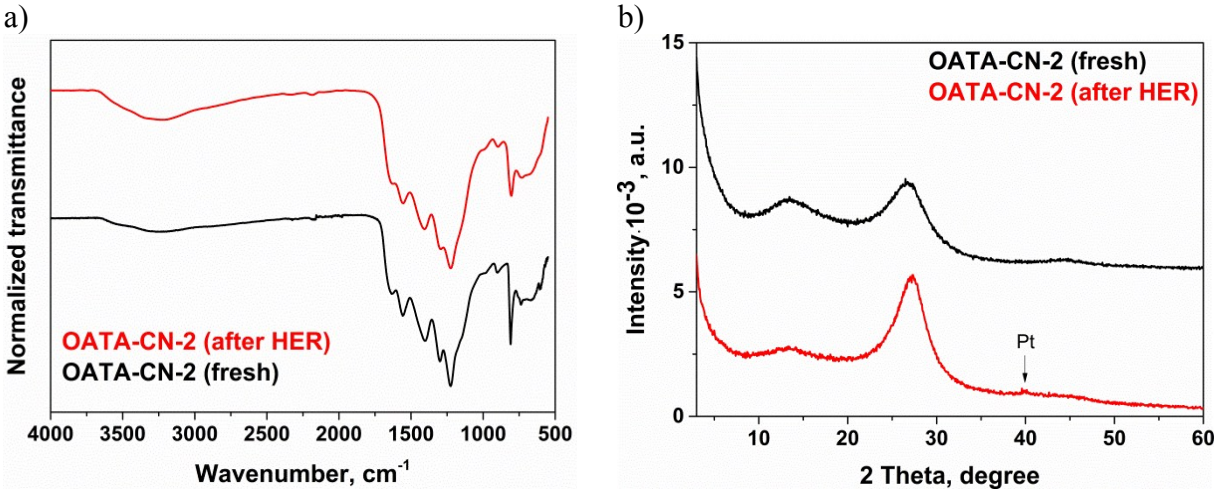

Figure S13. FTIR spectra (a) and PXRD patterns (b) of OATA-CN-2 before and after HER experiments, illustrating catalyst stability during photocatalytic tests.

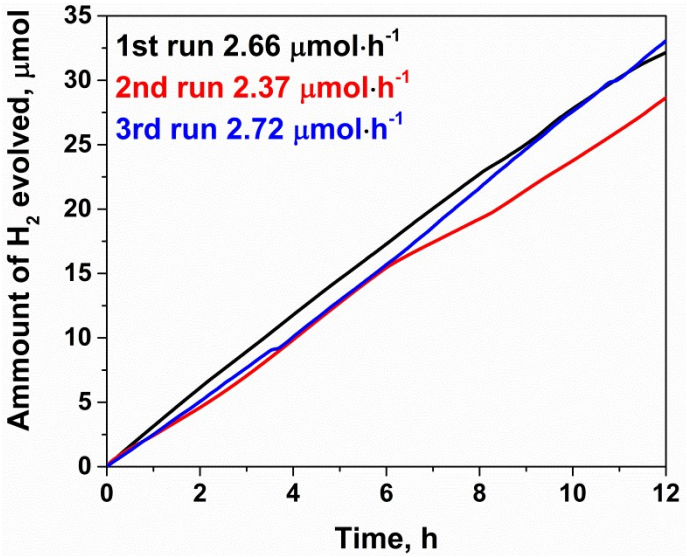

Figure S14. Time dependent Pt-assisted HER (using TEOA as a sacrificial holes scavenger and 50W white LED as an irradiation source) over OATA-CN-2 catalyst in three consecutive runs. In between the runs, the photocatalyst was collected by centrifugation, extensively washed with DI water and dried. Pt was photodeposited at the catalyst only during the first run.

Reference

[1] Krishnan, R. *Fundamentals of Semiconductor Electrochemistry and Photoelectrochemistry*; Wiley-VCH: Weinheim, Germany, 2007.